Available online at www.sciencedirect.com
ScienceDirect
Planetary and Space Science 56 (2008) 251–255
Planetary and Space Science
www.elsevier.com/locate/pss

The effect of ground ice on the Martian seasonal CO_2 cycle

Robert M. Haberle[a,*], Francois Forget[b], Anthony Colaprete[a], James Schaeffer[c], William V. Boynton[d], Nora J. Kelly[d], Matthew A. Chamberlain[d]

[a]*Space Science and Astrobiology Division, MS 245-3, NASA/Ames Research Center, Moffett Field, CA 94035, USA*
[b]*Laboratoire de Météorologie Dynamique, Institut Pierre Simon Laplace, Université Paris 6 BP99, 75252 Paris Cedex 05, France*
[c]*QSSS/Raytheon Corp., Palo Alto, CA, USA*
[d]*Deptartment of Planetary Sciences, University of Arizona, Tucson, AZ 85721, USA*

Available online 31 August 2007

Abstract

The mostly carbon dioxide (CO_2) atmosphere of Mars condenses and sublimes in the polar regions, giving rise to the familiar waxing and waning of its polar caps. The signature of this seasonal CO_2 cycle has been detected in surface pressure measurements from the Viking and Pathfinder landers. The amount of CO_2 that condenses during fall and winter is controlled by the net polar energy loss, which is dominated by emitted infrared radiation from the cap itself. However, models of the CO_2 cycle match the surface pressure data only if the emitted radiation is artificially suppressed suggesting that they are missing a heat source. Here we show that the missing heat source is the conducted energy coming from soil that contains water ice very close to the surface. The presence of ice significantly increases the thermal conductivity of the ground such that more of the solar energy absorbed at the surface during summer is conducted downward into the ground where it is stored and released back to the surface during fall and winter thereby retarding the CO_2 condensation rate. The reduction in the condensation rate is very sensitive to the depth of the soil/ice interface, which our models suggest is about 8 cm in the Northern Hemisphere and 11 cm in the Southern Hemisphere. This is consistent with the detection of significant amounts of polar ground ice by the Mars Odyssey Gamma Ray Spectrometer and provides an independent means for assessing how close to the surface the ice must be. Our results also provide an accurate determination of the global annual mean size of the atmosphere and cap CO_2 reservoirs, which are, respectively, 6.1 and 0.9 hPa. They also indicate that general circulation models will need to account for the effect of ground ice in their simulations of the seasonal CO_2 cycle.

Keywords: Mars; CO_2 cycle; Ground ice; Polar caps

1. Introduction

Understanding the state and distribution of water on Mars is fundamental to understanding of the evolution of the planet's climate system. The gamma ray spectrometer (GRS) experiment on the Mars Odyssey spacecraft has detected large abundances of hydrogen within a meter of the surface at middle and high latitudes in each hemisphere (Boynton et al., 2002; Mitrofanov et al., 2002; Feldman et al., 2002). The large abundances of hydrogen, ~70% water equivalent by volume, suggest it is most likely in the form of water ice, and models of the GRS observations suggest it is present in a layered configuration with relatively dry hydrogen-poor soil overlying an ice-saturated regolith (Boynton et al., 2002; Feldman et al., 2004; Prettyman et al., 2004). Here we show that this subsurface water ice acts as a thermal reservoir that provides enough heat to the surface during fall and winter to significantly affect the seasonal carbon dioxide (CO_2) cycle. Indeed, including this heat source in models of the CO_2 cycle eliminates the need for unrealistically low CO_2 frost emissivities, and provides an independent method for determining the depth to the water ice table that compliments the more traditional approach utilized by vapor diffusion models (Leighton and Murray, 1966; Farmer and Doms, 1979; Mellon and Jakosky, 1993; Schorghofer and Aharonson, 2005).

*Corresponding author. Tel.: +1 650 604 5491; fax: +1 650 604 6779.
E-mail address: Robert.M.Haberle@nasa.gov (R.M. Haberle).

0032-0633/$ - see front matter © 2007 Elsevier Ltd. All rights reserved.
doi:10.1016/j.pss.2007.08.006

2. Ground ice and the CO_2 cycle

The seasonal CO_2 cycle is defined by the exchange of CO_2 between two reservoirs: the atmosphere and polar caps. (Note that the thin permanent CO_2 ice cap at the South Pole is too small to have a significant effect on the seasonal cycle.) A third reservoir, adsorbed CO_2 on regolith grains (e.g., Zent et al., 1987), is not considered here since on seasonal time scales such a reservoir, if it exists at all, is not likely to experience significant change unless the pore sizes are unrealistically large (Toon et al., 1980). Thus, we consider only the atmosphere and cap system in which the exchange of CO_2 between them is driven by seasonal variations in the heat budget of polar regions (Leighton and Murray, 1966; Leovy and Mintz, 1969; Paige and Ingersoll, 1985; James et al., 1992).

The presence of subsurface water ice affects the seasonal CO_2 cycle by controlling the amount of heat conducted from the interior to the surface during the fall and winter seasons. With water ice in the ground, more of the solar energy absorbed at the surface during spring and summer is conducted down into the interior than if ice is absent. This heat is gradually released back to the surface during the fall and winter. The increased heat flux then reduces the amount of CO_2 that condenses on the ground. The magnitude of this effect depends on how much ice there is and how close to the surface it resides.

Fig. 1 illustrates the effect for a two-layer model in which dry Mars soil overlies an ice-rich regolith. The results are based on a 1-D version of the Ames general circulation model (GCM) running at 70°N with a two-layer soil model (soil overlying ice). The soil thermal inertia is 275 SI units, while the ice thermal inertia is 2200 SI with annual skin depths of approximately 1 and 5 m, respectively. It is the thermal conductivity that is responsible for the large difference in thermal inertia between soil and ice. The thermal inertia of the ice-rich regolith is consistent with values of pure ice or rock. In these simulations the surface heat balance does not include downward infrared radiation from the atmosphere or turbulent sensible heat exchange, and the atmosphere is assumed to be transparent to solar radiation. The conduction of heat in an ice-rich regolith is also responsible for seasonal variations in apparent thermal inertia (Chamberlain and Boynton, 2005), and leads to some improvement in modeled surface temperatures (Wilson and Smith, 2006).

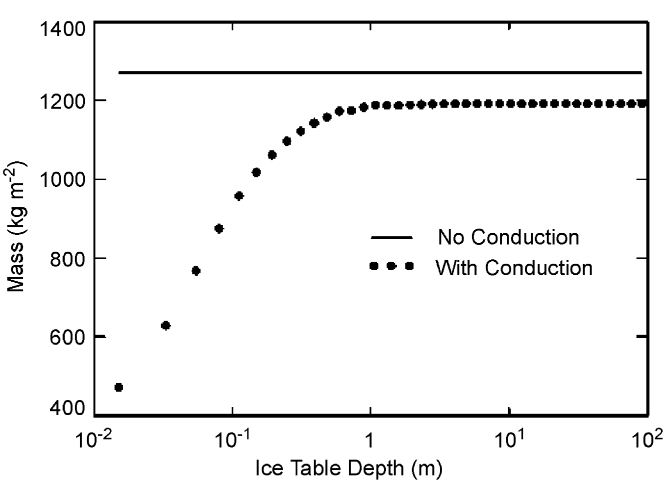

Fig. 1. The maximum CO_2 ice accumulation during a year as a function of ice table depth. The no-conduction curve corresponds to a simulation with zero thermal conductivity.

For ice table depths greater than ~1 m, the presence of ground ice has virtually no effect on the amount of CO_2 that condenses during fall and winter. However, as the ice table moves closer to the surface, less CO_2 condenses mostly because of the enhanced upward conducted heat flux. But there is also a feedback operating: CO_2 condenses later and sublimates earlier with ice close to the surface and this increases the time the surface is exposed to solar radiation and the energy available for subsurface storage. About three times less CO_2 condenses when the ice table is at the surface than when it is present at depths greater than a meter or so. Thus, the amount of CO_2 that condenses is very sensitive to the presence of ice close to the surface.

3. Modeling results

To further quantify this effect, we model the full seasonal CO_2 cycle using version 1.7.1 of the NASA/Ames Mars GCM (Haberle et al., 1999). This version is based on the UCLA B-grid running at 7.5° latitude by 9.0° longitude horizontal resolution, and 24 vertical layers from the surface to 0.0005 hPa (~80 km). It uses atmospheric heating algorithms that account for the radiative effects of dust and CO_2, and includes a full diurnal and seasonal cycle with a surface heat budget that includes the absorption of solar and infrared radiation from the atmosphere, infrared emission from the surface, turbulent sensible heat exchange, and subsurface heat conduction calculated from a layered soil model. The original soil model was modified to account for depth-dependent soil properties and its lower boundary was extended to 100 m. We run the model with a fixed dust loading (visible optical depth = 0.3) long enough for the CO_2 cycle to equilibrate (2 plus Mars years) and then analyze the last year.

We constrain the model with observations from the Viking and Odyssey missions. Surface pressure measurements at the two Viking Lander sites provide a measure of the size and variation of the global atmosphere reservoir (Hess et al., 1980). The reason for this is as follows. Strictly speaking, surface pressure is a measure of the local column mass loading and it is affected by elevation, atmospheric dynamics, and temperature variations in the atmosphere, as well as the growth and retreat of the polar caps (Hourdin et al., 1993, 1995). Thus, observations at only two points on the surface do not necessarily reflect global conditions. However, the elevation of the surface is now well known (Smith et al., 1999), and GCMs include the effects of dynamics and atmospheric temperature variations. Thus, in principle, a GCM that reproduces the

Viking pressure data can be used to infer the variations in the size of the global atmosphere reservoir.

Observations from Odyssey's GRS experiment provide constraints on the size and variation of the cap reservoirs (Kelly et al., 2006). The interaction of cosmic rays with Martian surface materials excites gamma-ray emission and neutron fluxes, which are modulated by seasonal variations in the overlying CO_2 mass loading. Specifically, the capture of slow moving neutrons by hydrogen atoms creates an excited state of deuterium, which emits gamma rays at 2.223 MeV during de-excitation. Inferences about the column density, spatial extent, and mass of the CO_2 polar caps, can be made from observations of the attenuation of this gamma ray line. The GRS observations extend over several Mars years and provide information on the size and variation of the polar caps in each hemisphere.

We show results from two simulations. In both simulations we adjust specific model parameters until a good fit to the Viking and Odyssey data is achieved. A good fit is defined as one in which the rms variation in daily averaged surface pressure integrated over the year (observed-modeled), and the offset between observed and modeled mean annual surface pressure is less than 0.1 hPa. The fitting is done by subjectively adjusting the total amount of CO_2 in the system (caps plus atmosphere), and the albedo and emissivity of the CO_2 cap in each hemisphere. For simplicity we assume the cap albedos and emissivities are constant in space and time, but can be different between hemispheres.

In the first simulation we fit the observations assuming there is no subsurface water ice. In the second simulation, we assume that subsurface water ice is present at latitudes and longitudes in accord with the GRS observations: roughly poleward of 55° in each hemisphere. (Note that there are longitudinal variations in the GRS observations, and these are included.) In these regions we assume that the ice-saturated regolith is overlain by soil whose albedo and thermal inertia can vary in latitude and longitude. We use the soil properties presently running in the Laboratoire de Météorologie Dynamique GCM (Forget et al., 1999), which are based on TES and Viking observations. For the ice layer, however, we assume that the depth to the ice and its thermal properties are independent of latitude and longitude and that the ice has the same thermal inertia as used in Fig. 1. Finally, and most importantly, we fix the CO_2 ice emissivity at unity, and instead vary the depth to the ice table when fitting the data. Table 1 summarizes the results of these two simulations. Figs. 2 and 3 show the fit to the Viking and GRS data. Note that we chose unit emissivity for the caps only to prove the concept. As illustrated in Fig. 4, the error in simulating the CO_2 cycle when running with unit emissivities is quite significant without ice in the ground.

Though the fitted simulations provide reasonable agreement with the data, we discount the simulation without subsurface water ice. In that run, the best-fit emissivities are unrealistically low. Such low emissivities would yield wintertime brightness temperatures near 125 K for the north cap, and 132 K for the south cap. Observed brightness temperatures typically exceed 140 K, though

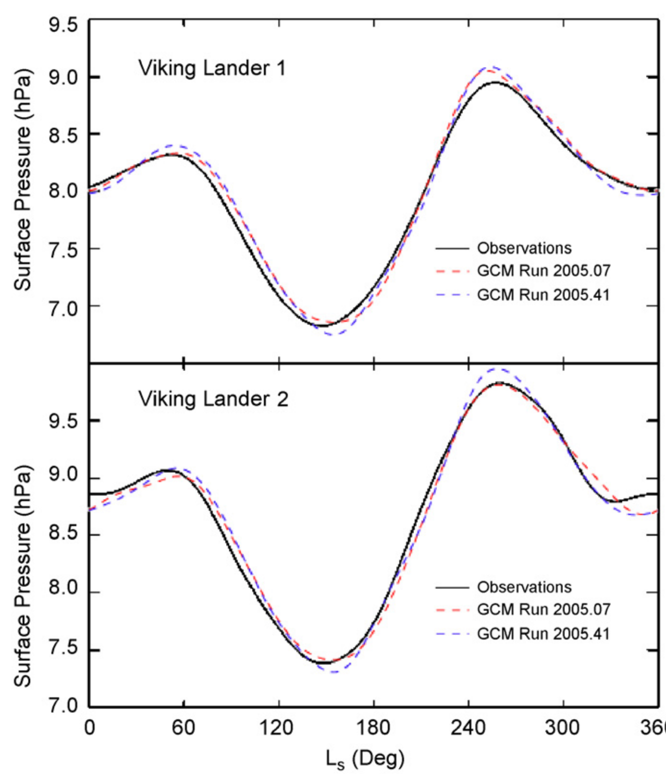

Fig. 2. Comparison of GCM simulated surface pressures (red and blue-dashed lines) at the two Viking Lander sites with the observations (black line). Both the observations and the GCM simulations have been daily averaged then fit to an eighth-order polynomial as described in Hourdin et al. (1995). The GCM surface pressures have been interpolated to the latitude and longitude of the Viking sites and have been corrected for elevation differences.

Table 1
Best-fit parameters for GCM runs

Run	Albedo	Emissivity[a]	Ice depth (cm)	Total CO_2 (hPa)	Atmosphere[b] (hPa)	Cap[b] (hPa)
2005.07: no subsurface water ice	0.7 (N)	0.5 (N)	Inf (N)	7.06	6.12	0.94
	0.5 (S)	0.7 (S)	Inf (S)			
2005.41: with subsurface water ice	0.6 (N)	1.0 (N)	8.05 (N)	7.04	6.13	0.91
	0.5 (S)	1.0 (S)	11.16 (S)			

[a]This is a fitting parameter only in Run 2005.07. It is fixed in run 2005.41.
[b]Annual and global mean.

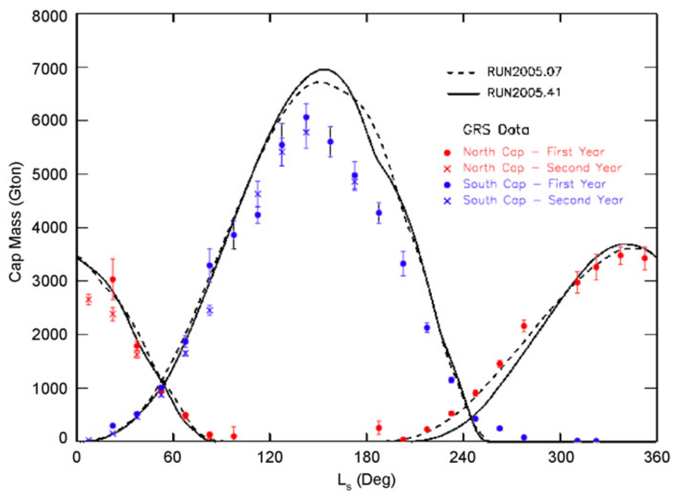

Fig. 3. Comparison of GCM simulated polar cap masses (full and dashed black lines) with GRS observations (red symbols for the North Cap, blue symbols for the South Cap). The GRS data are based on the hydrogen line, include error bars as indicated, and are further split out into first year data (solid circles) and second year data (crosses). See Prettyman et al. (2004) for details.

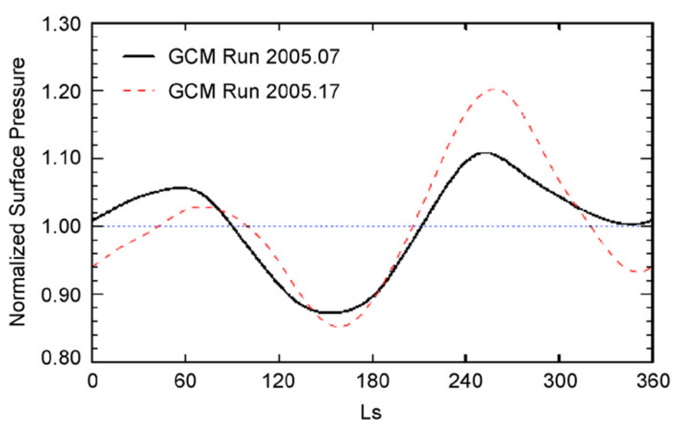

Fig. 4. Seasonal variation of the normalized global mean surface pressure for our best-fit simulation with no ground ice (run 2005.07), and the same run with unit cap emissivity in both hemispheres (run 2005.17).

they can be lower deep in the polar interior for limited times (Kieffer et al., 1977). Titus and Kieffer (2001) derived CO_2 frost emissivities that generally exceed 0.9, though they can be as low as 0.8 and sometimes even lower. Again, however, these low values are limited in space and time. Other models of the CO_2 cycle also require unrealistically low emissivities to fit the Viking data (James and North, 1982; Wood and Paige, 1992; Paige and Wood, 1992). The implication is that the models are missing a heat source, since they artificially suppress the frost radiative losses and hence the amount that condenses (see also Forget and Pollack, 1996). As shown in the run with subsurface water ice present, however, enhanced conduction from an ice-saturated regolith can provide that missing heat source while retaining more realistic cap emissivities. Furthermore, this run provides an estimate to the average depth of the ice table in each hemisphere: ~8 cm in the Northern Hemisphere and ~11 cm in the Southern Hemisphere. (Note that the additional significant figures shown in Table 1 are a consequence of our numerical grid set up, and are not an indication of extreme sensitivity.) For a soil density of $2\,g\,cm^{-3}$, this corresponds to a mass loading of the hydrogen-poor layer of $16\,g\,cm^{-2}$ for the north, and $22\,g\,cm^{-2}$ for the south, which is consistent with models of the GRS data (Boynton et al., 2002; Feldman et al., 2004; Prettyman et al., 2004; Litvak et al., 2006). This hemispheric asymmetry in the depth to the ice table is also consistent with the difference between the best-fit north and south cap emissivities in the no-subsurface-water-ice run, i.e., a shallower ice table in the north is equivalent to requiring a lower best fit emissivity in the absence of ground ice.

4. Discussion

Several additional points are worth mentioning. First, these results provide the best quantitative estimates to date of the size of the global atmosphere/cap system: to within 0.1 hPa (our best-fit offset criterion) the global mean annual "sea level" pressure on Mars is about 6.1 hPa, and the global mean annual size of the cap reservoir is about 0.9 hPa. More precise estimates of these important quantities may be possible with further analyses of the GRS and Viking data (Boynton et al., 2006).

Second, we note that our best-fit cap albedos, emissivities, and depth to ground ice are not unique. There are a variety of combinations of these parameters that could fit the Viking and Odyssey data. Indeed our best-fit cap albedos are somewhat higher than observed by TES. The best approach here would be to constrain the cap properties from TES observations, and then fit the Viking and Odyssey data by adjusting the depth to ground ice. This is, in fact, our plan. Our motivation here is to simply demonstrate that the low emissivity problem is significantly mitigated by the inclusion of ground ice in the polar energy budget, and that by constraining the model to reproduce the Viking an Odyssey data it is possible to infer the depth to ground ice.

Third, it is important to emphasize that the ice table depths estimated here are spatially uniform in contrast to those calculated from vapor diffusion models and what would be expected in reality. Furthermore, they should also be viewed as preliminary since we have made some simplifying assumptions (e.g., constant cap properties and dust loading), and they are very sensitive to the thermal inertia of the dry soil, which may be lower than inferred from Viking/TES data at high northern latitudes ($>80°$) where diurnal thermal inertias can exceed 500 SI. In these regions the diurnal skin depth is comparable to our inferred ice table depth. If our two layer soil model is valid, then the "dry" layer overlying the ice must have a lower thermal inertia than inferred from the Viking/TES data in which case we would be underestimating the depth to ground ice in these regions. If it is not, i.e., the soil is homogeneous, then we would probably require lower CO_2 cap emissivities at these locations to fit the data. However, the regions where the diurnal skin depth is comparable to the ice table depth are limited to the very high northern latitudes. Consequently, they have a small effect on the CO_2 cycle and would not change our conclusions regarding the "missing heat source". In general, our results suggest that ice must be close to the surface (within a seasonal skin depth), and that it is generally closer to the surface in the Northern Hemisphere than in the Southern Hemisphere.

There are of course some differences between the simulations and observations. Most notable is the greater than observed simulated cap mass in the Southern Hemisphere, which partly explains why the simulated pressure data have slightly greater amplitudes than is seen in the Viking data. But these differences are minor compared to the good overall agreement, and may be improved by including spatial and temporal variations in key parameters such as cap albedos and emissivities, ice table depth, and atmospheric dust and clouds whose radiative effects could be more important than we have assumed here (Wilson et al., 2007). Constraining model ground temperatures with observations should also improve the results. Such studies are underway and will be reported on in subsequent papers. But for now, it is clear that future models of the CO_2 cycle will need to account for the effects of subsurface water ice in order to run with realistic emissivities, and that such models can provide an independent estimate of the ice table depth. It is quite amusing that measurements of surface pressure, which are primarily used for atmospheric studies, can also be used to constrain the depth and distribution of subsurface ground ice on Mars.

Acknowledgments

We thank Chris McKay and Aaron Zent for helpful comments in preparing this manuscript. We also thank R. John Wilson and an anonymous reviewer for providing constructive reviews. NASA's Mars Data Analysis and Planetary Atmospheres programs supported this work.

References

Boynton, W.V., et al., 2002. Distribution of hydrogen in the near surface of Mars: evidence for subsurface ice deposits. Science 297, 81–85.

Boynton, W.V., Haberle, R., Kelly, N. Sprague, A., 2006. Use of Mars Odyssey GRS results to constrain the exchangeable mass of Martian CO_2. In: Forget, F., et al. (Eds.), Second Workshop on Mars Atmosphere Modeling and Observations, Granada, Spain.

Chamberlain, M.A., Boynton, W.V., 2005. Effect of ground ice on apparent thermal inertia on Mars. In: Proceedings of 36th Lunar and Planetary Science Conference, No. 1566.

Farmer, C.B., Doms, P.E., 1979. Global seasonal variation of water vapor on Mars and the implications of permafrost. J. Geophys. Res. 84, 2881–2888.

Feldman, W.C., et al., 2002. Global distribution of neutrons from Mars: results from Mars Odyssey. Science 297, 75–78.

Feldman, W.C., et al., 2004. Global distribution of near-surface hydrogen on Mars. J. Geophys. Res. 109, E09006.

Forget, F., Pollack, J.B., 1996. Thermal infrared observations of the condensing Martian polar caps: CO_2 ice temperatures and radiative budget. J. Geophys. Res. 101, 16,865–16,879.

Forget, F., et al., 1999. Improved general circulation models of the Martian atmosphere from the surface to above 80 km. J. Geophys. Res. 104, 24155–24176.

Haberle, R.M., et al., 1999. General circulation model simulations of the Mars Pathfinder atmospheric structure investigation/meteorology data. J. Geophys. Res. 104, 8957–8974.

Hess, S.L., Ryan, J.A., Tillman, J.E., Henry, R.M., Leovy, C.B., 1980. The annual cycle of pressure on Mars measured by Viking Landers 1 and 2. Geophys. Res. Lett. 7, 197–200.

Hourdin, F., Le van, P., Forget, F., Talagrand, O., 1993. Meteorological variability and the annual surface pressure cycle on Mars. J. Atmos. Sci. 50, 3625–3640.

Hourdin, F., Forget, F., Talagrand, O., 1995. The sensitivity of the Martian surface pressure and atmospheric mass budget to various parameters: a comparison between numerical simulations and Viking observations. J. Geophys. Res. 100, 5501–5523.

James, P.B., North, G.R., 1982. The seasonal CO_2 cycle on Mars—an application of an energy balance climate model. J. Geophys. Res. 87, 10271–10283.

James, P.B., Kieffer, H.H., Paige, D.E., 1992. The seasonal cycle of carbon dioxide on Mars. In: Kieffer, H.H., et al. (Eds.), Mars. University of Arizona Press, Tucson, AZ, pp. 934–968.

Kelly, N.A., et al., 2006. Seasonal polar carbon dioxide frost on Mars: CO_2 mass and columnar thickness distribution. J. Geophys. Res. 111, E03S07.

Kieffer, H.H., et al., 1977. Thermal and albedo mapping of Mars during the Viking primary mission. J. Geophys. Res. 82, 4249–4291.

Leighton, R.R., Murray, B.C., 1966. Behavior of carbon dioxide and other volatiles on Mars. Science 183, 136–144.

Leovy, C.B., Mintz, Y., 1969. Numerical simulation of the weather and climate of Mars. J. Atmos. Sci. 26, 1167–1190.

Litvak, M.L., et al., 2006. Comparison between polar regions of Mars from HEND/Odyssey data. Icarus 180.

Mellon, M.T., Jakosky, B.M., 1993. The distribution and behavior of Martian ground ice during past and present epochs. J. Geophys. Res. 100, 11781–11799.

Mitrofanov, I.G., et al., 2002. Maps of subsurface hydrogen from the High Energy Neutron Detector, Mars Odyssey. Science 297, 78–81.

Paige, D.A., Ingersoll, A.P., 1985. Annual heat balance of Martian polar caps—Viking observations. Science 228, 1160–1168.

Paige, D.A., Wood, S.E., 1992. Modeling the Martian seasonal CO_2 cycle 2. Interannual variability. Icarus 99, 15–27.

Prettyman, T.H., et al., 2004. Composition and structure of the Martian surface at high southern latitudes from neutron spectroscopy. J. Geophys. Res. 109, E05001.

Schorghofer, N., Aharonson, O., 2005. Stability and exchange of subsurface ice on Mars. J. Geophys. Res. 110, E05003.

Smith, D.E., et al., 1999. The global topography of Mars and implications for surface evolution. Science 284, 1495–1498.

Titus, T.N., Kieffer, H.H., 2001. TES premapping data: slab ice and snow flurries in the Martian north polar night. J. Geophys. Res. 106, 23181–23196.

Toon, O.B., Pollack, J.B., Ward, W., Burns, J.A., Bilski, K., 1980. The astronomical theory of climatic change on Mars. Icarus 44, 552–607.

Wilson, R.J., Smith, M.D., 2006. The effects of atmospheric dust on the seasonal variation of Martian surface temperature. In: Proceedings of Second Workshop on Mars Atmosphere Modeling and Observations, Granada, Spain.

Wilson, R.J., Neumann, G.A., Smith, M.S., 2007. The diurnal variation and radiative influence of Martian water ice clouds. Geophys. Res. Lett. 34, L02710.

Wood, S.E., Paige, D.A., 1992. Modeling the Martian seasonal CO_2 cycle. 1. Fitting the Viking Lander pressure curves. Icarus 99, 1–14.

Zent, A.P., Fanale, F.P., Postawko, S.E., 1987. Carbon dioxide—adsorption on palagonite and partitioning in the Martian regolith. Icarus 71, 241–249.